

Article

# Conception and Evolution of the Probabilistic Methods for Ship Damage Stability and Flooding Risk Assessment

Dracos Vassalos \* and M. P. Mujeeb-Ahmed

Maritime Safety Research Centre (MSRC), Department of Naval Architecture, Ocean and Marine Engineering, University of Strathclyde, Glasgow G4 0LZ, UK; mujeeb.mughadar-palliparambil@strath.ac.uk

\* Correspondence: d.vassalos@strath.ac.uk

**Abstract:** The paper provides a full description and explanation of the probabilistic method for ship damage stability assessment from its conception to date with focus on the probability of survival (s-factor), explaining pertinent assumptions and limitations and describing its evolution for specific application to passenger ships, using contemporary numerical and experimental tools and data. It also provides comparisons in results between statistical and direct approaches and makes recommendations on how these can be reconciled with better understanding of the implicit assumptions in the approach for use in ship design and operation. Evolution over the latter years to support pertinent regulatory developments relating to flooding risk (safety level) assessment as well as research in this direction with a focus on passenger ships, have created a new focus that combines all flooding hazards (collision, bottom and side groundings) to assess potential loss of life as a means of guiding further research and developments on damage stability for this ship type. The paper concludes by providing recommendations on the way forward for ship damage stability and flooding risk assessment.



**Citation:** Vassalos, D.; Mujeeb-Ahmed, M.P. Conception and Evolution of the Probabilistic Methods for Ship Damage Stability and Flooding Risk Assessment. *J. Mar. Sci. Eng.* **2021**, *9*, 667. <https://doi.org/10.3390/jmse9060667>

Academic Editors: Kostas J. Spyrou, Apostolos Papanikolaou and Alessandro Antonini

Received: 13 May 2021  
Accepted: 9 June 2021  
Published: 16 June 2021

**Publisher's Note:** MDPI stays neutral with regard to jurisdictional claims in published maps and institutional affiliations.



**Copyright:** © 2021 by the authors. Licensee MDPI, Basel, Switzerland. This article is an open access article distributed under the terms and conditions of the Creative Commons Attribution (CC BY) license (<https://creativecommons.org/licenses/by/4.0/>).

**Keywords:** ship damage stability; probabilistic methods; flooding risk

## 1. Introduction

The main ideas for probabilistic damage stability assessment as embedded in SOLAS (safety of life at sea) 2009/2020, are based on the fundamental assumption that the ship under investigation is damaged with ensuing large-scale flooding stemming from hull breach (collision is the only hazard presently being considered). This can be regarded as the conditional probability of losing ship stability in the wake of a collision event only, ignoring among others the area of operation and hence operating environment, type of ship, type and size of breach, technology, crew onboard. More importantly, the time element, hence evacuation arrangements and associated Risk Control Options (RCOs) are being overlooked [1]. This said, many risk-related factors such as size of ship, number of persons on board, lifesaving appliances, subdivision and other arrangements are accounted for by the Required Index of Subdivision,  $R$ . This plays a vital role within the probabilistic framework, as provided by the inequality (1), where  $A$  is the probability of ship surviving collision damage, namely the Attained Subdivision Index.

$$A \geq R \quad (1)$$

The Attained subdivision index as outlined within SOLAS 2009 [2], is shown in Equation (2) below.

$$A = \sum_{j=1}^J \sum_{i=1}^I w_j \cdot p_i \cdot s_i \quad (2)$$

where:

$j$  represents the loading condition under consideration.

$J$  represents the total number of loading conditions considered in the calculation of  $A$ , usually three draughts covering the operational draught range of the vessel.

$w_j$  represents a weighting factor applied to each initial draught.

$i$  represents each compartment or group of compartments under consideration for loading condition,  $j$ .

$I$  is the total number of all feasible damage scenarios involving flooding of individual compartments or groups of adjacent compartments.

$p_i$  is the probability that, for loading condition,  $j$ , only the compartment or group of compartments under consideration are flooded, disregarding any horizontal subdivision.

$s_i$  accounts for the conditional probability of survival following flooding of the compartment or group of compartments under consideration for loading condition  $j$  weighted by the probability that the space above a horizontal subdivision may not be flooded.

In this respect, the Attained Subdivision Index represents the conditional “averaged” probability of survival or else the “weighted average s-factor”, as depicted in Equation (3).

$$A = E(I) \quad (3)$$

Using different wording, Index  $A$  is the marginal probability for time to capsize within a certain time, assuming that the time being considered is sufficiently long for capsize to have occurred in most cases. Finally, the Required Index of Subdivision,  $R$ , represents the level of safety associated with collision and flooding events that is deemed to be acceptable by society, in the sense that it is derived using ships, which society considers fit for purpose, since they are in daily operation. In line with the standards in place, the Attained Index must be greater than the required  $R$  ( $A > R$ ) and specifically for passenger ships ( $A \geq 0.9R$ ) to form the limiting metacentric height or GM curves. There are two key elements in Equation (2) which have been the focus of research ever since Wendel has proposed the probabilistic framework for damage stability assessment [3,4], commonly referred to as the s-factor and the p-factor. The first will be the focus of attention in this paper. For a more in-depth understanding of the second as well as a complete up to date developments, see [5].

## 2. S-Factor Definition

### 2.1. Capsize Band

In assessing the ability of a ship to survive a damaged state in a random wave environment, answers to two questions are sought: (a) probability to survive or capsize in each sea state [6] and, (b) given the latter, the time that it takes for this to happen. The second is such a basic question but it was not until the mid-1990s (North West European Project), where the capsize band concept, [7–9], offered the basis for a credible answer. In simple terms, the capsize band describes the transition of sea-states from those at which no capsize is observed (lower boundary) to those at which the probability of capsize equals unity (upper boundary). This is a region outside which capsize is either unlikely to happen or certain. The capsize band can be depicted in two ways: through the variation of the KG or the GM for different sea states. One example of the latter is provided in Figure 1.

The capsize band indicates the range of sea states within which a transition from unlikely ( $P_s = 1/P_c = 0$ ) to certain capsize ( $P_c = 1/P_s = 0$ ) can be observed, where  $P_s$  and  $P_c$  represents probability of survival and capsize, respectively. The width of the capsize band reflects the variation of the damage characteristics and ship loading conditions. Even though the capsize band is depicted in the form of confidence intervals, in fact, it measures the dispersion of capsizes, which in turn relates to separate sea states for which the capsize rate (i.e., the conditional probability of capsize) is very low from those in which the rate is very high. Allied to this, the capsize band signifies that there is no distinct boundary that separates safe from unsafe sea states, but instead a transition zone within which capsize is possible. Even though there are sea states that the vessel always survives and sea states that the vessel will inevitably always capsize, the lower and upper capsize/survival boundaries can be represented by means of limits. In this case, this asymptotic nature requires the

use of threshold values of the conditional probability outside of which the occurrence of capsize will either be impossible or practically certain.

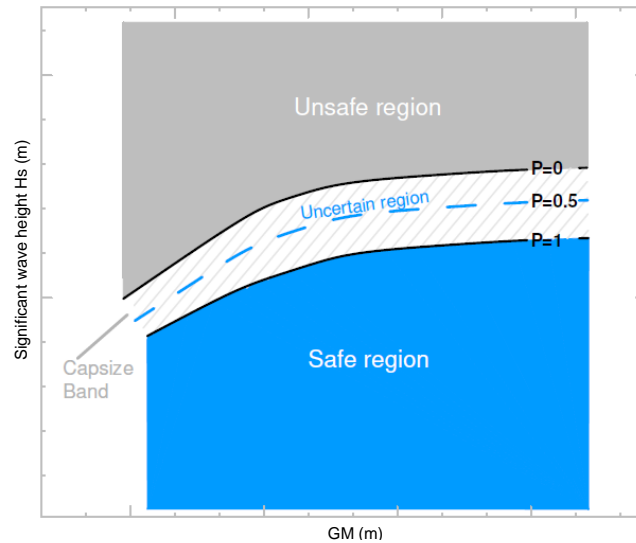


**Figure 1.** Capsize band with the indication of safe, uncertain and unsafe regions (one damage scenario in different loadings conditions and sea states).

Figure 2 represents a sample of capsize rates for various simulation times, forming a sigmoid shape distribution. The rate of observed capsizes is depended upon the time of observation and, in case of the limiting case of infinite exposure, the capsize rate distribution will turn into a unit step function, as indicated in Figure 2 for increased simulation times. In this vein, for a small number of capsize probability, the corresponding significant wave height will remain the same (with only minor difference) with time of observation. In other words, a sea state corresponding to a small capsize rate can be established on the basis of relatively short simulations and would remain valid for longer observations.

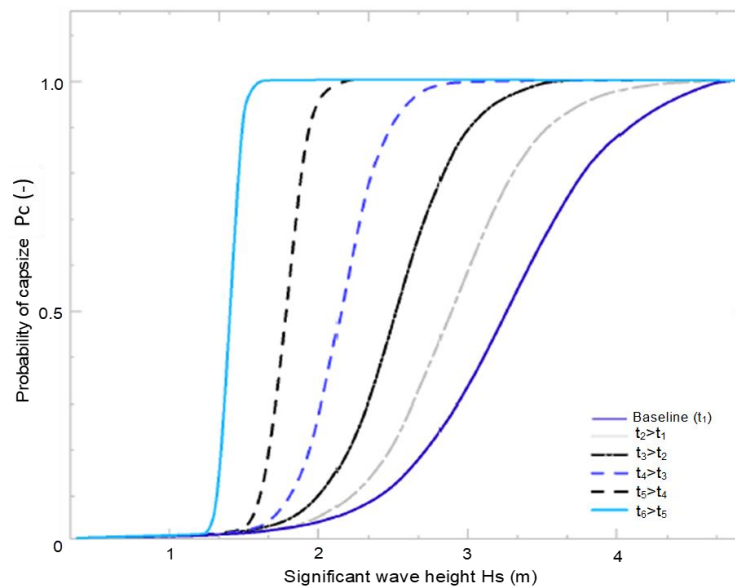


**Figure 2.** Change in shape of the capsize band with increasing exposure time  $t_1$  for the baseline scenario (dark blue line). The capsize rate is derived for one damage, one loading condition and varying significant wave heights.

### 2.2. Critical Significant Wave Height

In line with the probabilistic framework of assessing damage stability, the fundamental element, which describes the probability of surviving collision damages in waves, is described by the *s*-factor as depicted by Equation (4). The relationship between the survivability factor and the critical wave height stems from the consideration of the *s*-factor as an average probability of survival, with the averaging function being the probability density function of the encountered sea states during collision incidents as provided by Equation (4), [2,10,11].

$$s = \text{Prob}\{H_s \leq H_{s_{crit}}\} = \int_0^{\infty} f_c(H_s) \cdot P(H_s) \cdot dH_s \tag{4}$$

where:

$f_c(H_s)$  = probability density function of sea states recorded at the instance of collision.

$P(H_s)$  = probability of surviving flooding casualty in sea states for a specific time given the specific loading condition and flooding extent.

Furthermore, it can be assumed that  $P(H_s)$  is a unit step function centred at the critical or limiting  $H_s$  (i.e.,  $P(H_s) = 1$  for all  $H_s \leq H_{s_{crit}}$  and 0 otherwise), hence the *s*-factor can be expressed as follows:

$$s = \text{Prob}\{H_s \leq H_{s_{crit}}\} = \int_0^{H_{s_{crit}}} f_c(H_s) \cdot dH_s \tag{5}$$

The above suggests that to evaluate the factor *s*, it is necessary to establish the critical (or limiting) sea state  $H_{s_{crit}}$ . It should be noted that, with the tests performed during the *s*-factor development being limited to 30 min, the probability of survival is in fact a conditional probability, yielding:

$$s(t = 30\text{min}) = \int_0^{\infty} dH_s \cdot f_c(H_s) \cdot P_{surv}(t = 30\text{min}|s) \tag{6}$$

It should be noted that although replacing the probability distribution with a step function, is supported by little evidence, it does the “trick” and allows avoiding integration with little impact on the accuracy of the prediction, as long as the bandwidth of the capsize band is narrow. In this respect, the main problem deriving from the need of accurately predicting the critical significant wave height is a major flaw of the SOLAS 2009 *s*-factor formulation (although not readily obvious in the regulation). Eventually, the final formulation becomes:

$$s = \int_0^{H_{s_{crit}}} dH_s \cdot P_{H_s|coll}(H_s) = \exp(-\exp(0.16 - 1.2H_{s_{crit}})), \tag{7}$$

where  $H_{s_{crit}}$  is given as:

$$H_{s_{crit}}|_{t=30\text{min}} = 4 \left( \frac{\min(GZ_{max}, 0.12)}{0.12} \cdot \frac{\min(Range, 16)}{16} \right) = 4s(t = 30\text{min})^4 \tag{8}$$

This approach, adopted within the GOALDS (Goal-Based Damage Stability) project [12], is similar to that of the HARDER (Harmonisation of Rules and Design Rationale) project, [13], with the main difference stemming from the assumption of  $H_{s_{crit}}$  corresponding to the lower limit of the capsize band, thus allowing for a justified assumption of very long (“infinite”) time of survival.

Notwithstanding this, the critical sea state for a specific damage extent and loading condition can be established either with the aid of model test experiments or employing time-domain numerical simulations. Both approaches have been utilised in the past in the course of the development and verification of survivability criteria. Generally, the experiments, either of physical or numerical nature, are subjected to repeated time trials (usually 30 min full-scale) in a random realisation of a specific sea state with the view to deriving the capsizing rate at that specific wave height. A distribution  $P(H_s)$  can then be derived, following multiple repetitions of tests, [9]. Depending on the definition, the critical sea state can be regarded as a wave height at which  $P(H_s) = 0.5$  or, alternatively, as the highest sea state with a low probability of capsizing (e.g.,  $P(H_s) < 0.05$ ), as proposed in GOALDS [12] and more in-line with the notion of limiting wave height, as explained in [14].

Normally, the critical wave height is related to the geometrical characteristics of the vessel and its residual stability. These, of course, vary depending on the derivation process and design of experiments implemented. Customarily, this step is implicitly considered with the s-factor calculations. In this sense, the s-factor eclipses the presence of the critical sea state and instead, survivability is expressed directly as a function of ship stability residual parameters. This history of the related development is presented next.

### 3. S-Factor Evolution

#### 3.1. IMO (International Maritime Organization) Resolution A.265

The survivability factor adopted in resolution A.265 [15] is based on an extensive experimental research on survivability, [16]. Historically, that was the second time model experiments were conducted on a flooded ship model, the first being by Middleton and Numata in 1970 [17], aimed at identifying relationships that characterise the survival sea state of a ship damage case as a function of residual stability parameters, as shown in Figure 3. The formulation for the survivability factor as later adopted by IMCO (Inter-Governmental Maritime Consultative Organization) [15], in a slightly modified approximate format is shown in Equation (9).

$$s = 4.9 \sqrt{\frac{F_E \cdot GM}{B}} \quad (9)$$

where:

$F_E$  = equivalent residual freeboard (m).

$GM$  = initial stability (flooded metacentric height) (m).

$B$  = breadth of the ship (m).

The process of deriving the s-factor for the given damage condition underlying damage stability calculations in A.265 is illustrated in Figure 3. Simply, using different damaged GMs (one GM is presented below) leads to an approximation of the survival state obtained through the cumulative probability of survival. Unfortunately, like in the case for Rahola, using global ship parameters to establish a relationship between residual stability and sea state has influenced adversely almost every subsequent attempt to refine this, which for the case of passenger ships with complex internal environments it provides a wrong focus, as explained later.

#### 3.2. Static Equivalent Method (SEM)

Historically, SEM is an approach originally recommended based on many model test observations, e.g., [18,19]. Deriving from the findings of the HARDER Project, it was suggested that SEM should be used for the estimation of survivability in waves of RoRo ships while the conventional s-factor should be used for the estimation of survivability of cargo ships.

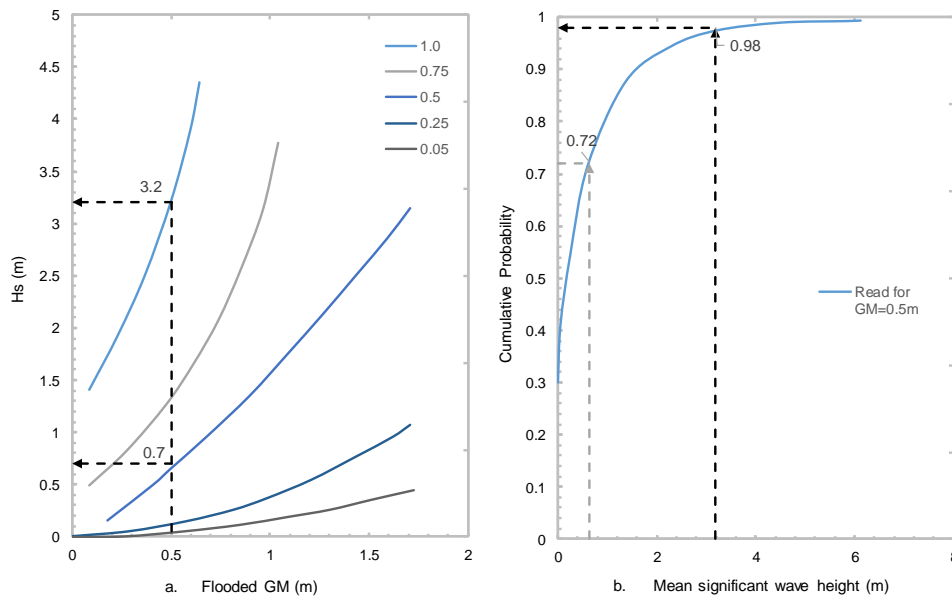


**Figure 3.** Method of deriving limiting sea-state and survival index  $s$ : (a)  $H_s$  vs. flooded GM for different freeboards (for example at flooded GM = 0.5 and freeboard = 1.0 m), limiting  $H_s = 3.2$  m. For the same flooded GM and freeboard = 0.5 m, limiting  $H_s = 0.7$  m; (b) cumulative probability distribution (CPD) of  $H_s$  at occurrence of capsizing (from accident statistics). At  $H_s = 3.2$  m, the probability is 0.98 (hence exceedance probability 0.02) and at  $H_s = 0.7$  m, the probability is 0.72 (hence exceedance probability 0.28).

Notably, as mentioned in [20], the SEM methodology was developed on the basis that the traditional survivability methods (residual GZ parameters) do not adequately estimate survivability of RoRo ships. At the time, a distinction was made between low freeboard Ro-Ro vessels and non-RoRo vessels, because of the observed differences in their mechanisms of capsizing, pertinent to these ships. The original SEM method linked the critical sea state to ship performance in waves (dynamic elevation of floodwater resulting from action of waves on the vehicle deck,  $h$ ), applicable only to RoRo vessels with large undivided spaces on the like vehicle decks, as shown in Equation (10), Figure 4.

$$H_{s_{crit}} = \left( \frac{h}{0.085} \right)^{\frac{1}{1.3}} \tag{10}$$

where both the  $H_{s_{crit}}$  and  $h$  are taken as median values of the respective random quantities. The critical significant wave height can then be used in the  $s$ -factor formulation, adopting the cumulative distribution of waves from IMO.

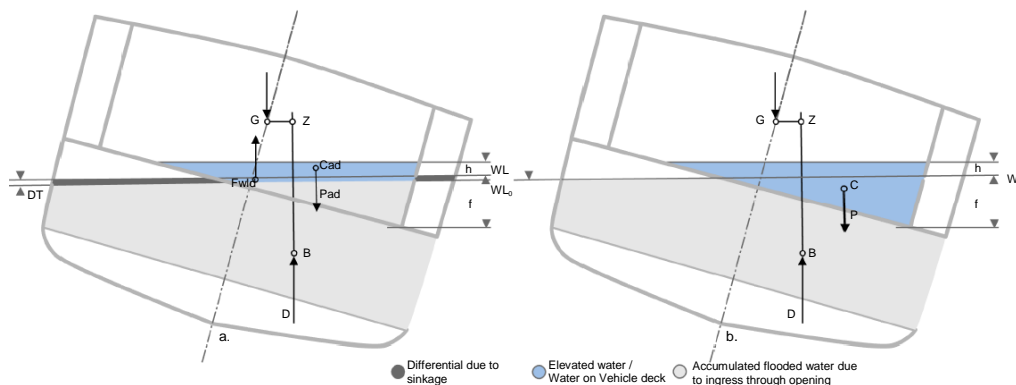


**Figure 4.** (a) Depiction of SEM parameters with water elevation in the vehicle deck at the Point of No Return (PNR)-case of RoRo ship; (b) normal method employed by damage stability software considering the floodwater volume as a total water on the vehicle deck inside an undamaged tank [21].

In project HARDER, the formulation was updated following a statistical relationship between dynamic water head ( $h$ ), the freeboard ( $f$ ), the critical heel angle and the mean significant survival wave height.

### 3.3. SOLAS 2009

Damage stability in SOLAS 2009 is calculated based on the findings of project HARDER by means of the s-factor as a metric of the safety level for statutory compliance, using cargo ships. Figure 5 shows all the related parameters, which are involved in the calculation of the s-factor and Index-A according to SOLAS II-1 §7-2.

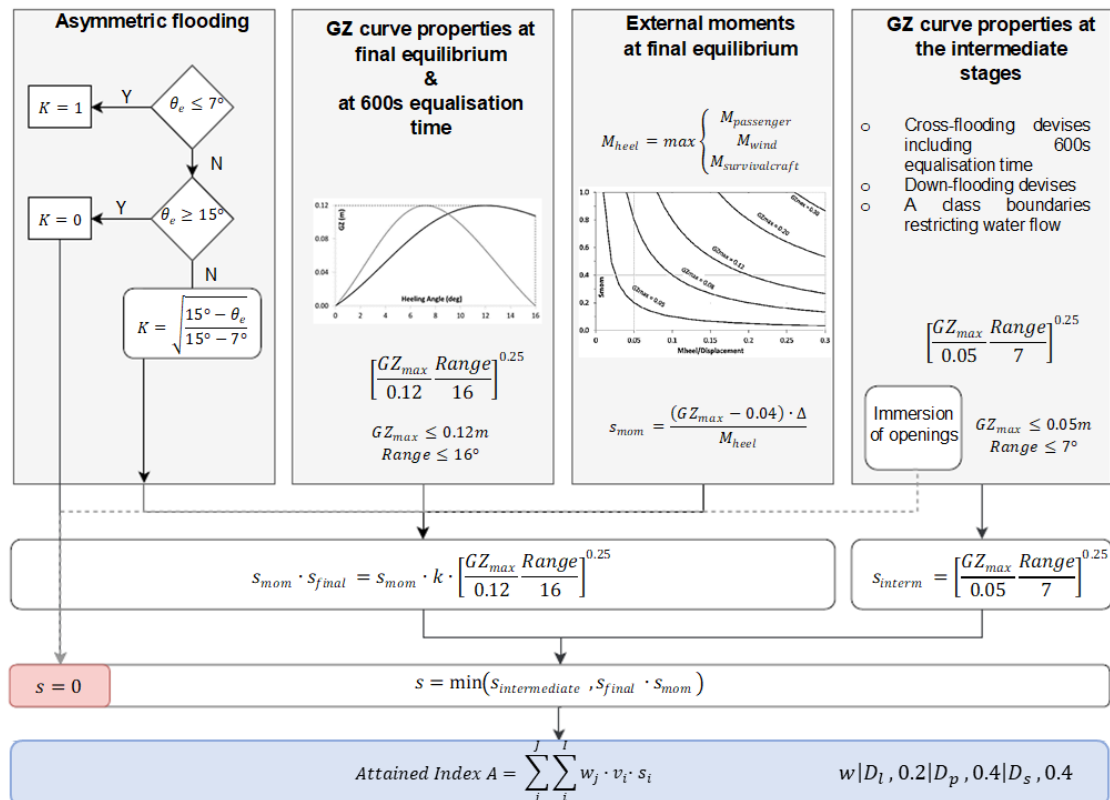


**Figure 5.** Calculation process of s-factor as per SOLAS 2009 accounting for external moments ( $M$ ) at final and intermediate stages of flooding ( $\theta_e$ —equilibrium heel angle;  $GZ_{max}$ —maximum positive righting lever;  $Range$ —range of positive righting lever;  $M_{heel}$ —heeling moment;  $M_{wind}$ —wind moment;  $M_{passenger}$ —heeling moment due to the movement of passengers;  $M_{survivalcraft}$ —heeling moment due to the launching of all fully loaded davit-launched survival craft on one side of the ship;  $s_{intermediate}$ —probability to survive all intermediate flooding stages until the final equilibrium stage;  $s_{final}$ —probability to survive in the final equilibrium stage of flooding;  $s_{mom}$ —probability to survive heeling moments;  $D_l, D_p, D_s$  represents deepest subdivision draught, light service draught and partial subdivision draught, respectively).

The coefficients of 0.12 m and 16 degrees are regression parameters, usually referred to as targeting values  $TGZ_{max}$  and  $TRange$ , respectively. As in the case of resolution A.265, the probability of survival of a flooding event after a collision damage involving one or more compartments is currently defined in SOLAS Ch.II-1 Regulation 7-2 through the s-factor. The formulation of the s-factor is also based on the concept of critical significant wave height  $H_{s_{crit}}$ , as derived from HARDER project, [22], and explained earlier.

$$H_{s_{crit}} = 4 \cdot \frac{GZ_{max}}{0.12} \cdot \frac{Range}{16} = 4s^4 \leftrightarrow s = \left( \frac{H_{s_{crit}}}{4} \right)^{0.25} \tag{11}$$

It is noteworthy to mention that the survival factor established through harmonisation in probabilistic rules, produced a survival probability relating to the dynamic effects of

encountering waves only when the vessel had reached final equilibrium after damage. In addition to using some old cargo ships for the derivation of an Index for universal application, there are many pitfalls in its derivation, especially with reference to passenger ships, for example [23–29]. These have been “ironed out” in the attempts to produce harmonised regulations between cargo and passenger ships, until project eSAFE (enhanced stability after a flooding event) brought attention to some of these problems, [30], which are being attended to in project [31].

### 3.4. EMSA (European Maritime Safety Agency) 2009

The EMSA project on the investigation of survivability of different ships [10,11], focused on the impact of the different parameters of the framework. In this sense, a new formulation is not proposed but instead a recommendation is brought forward to change the SOLAS targeting values for  $GZ_{\max}$  and *Range* to 0.25 m and 25 degrees, respectively, which by all accounts seem to be capturing the RoPax survivability with sufficient accuracy. However, despite the attempts of the EMSA study to address an accurate survivability factor for passenger ships, the drawbacks of the formulation are not diminished with application to cruise ships. To this end, a call for further improvements led to project GOALDS [12], aiming to cater for passenger ships whilst accounting for the main differences between RoPax and cruise ships.

### 3.5. GOALDS Project

As part of this project, 20 RoPax damages and 2 cruise ships were subjected to parametric investigation numerically, [14], for the establishment of survivability, whereas experiments in modern water basins were conducted on two RoPax and two cruise ships, respectively, for verification purposes in collision damages. For this, worst SOLAS 2-compartment damage were used  $\pm 35\%$ L amidships, whilst, for the case of cruise ships, which exhibited high resistance to capsize, 3-compartment damages were used for the derivation of the survivability boundary, [14]. The study presented in [14] concluded that the two stability parameters in the current survivability formulation, namely  $GZ_{\max}$  and *Range* are insufficient in capturing the relationship between the critical wave height and residual stability and, as a result, an additional element was identified reflecting ship size. In this respect, the centroid of the residual volume as a function of the vertical centres of intact and damaged compartments divided by the draft of the intact condition was used to compensate for the size parameter. This is the second attempt, the first one being Equation (10), to account for ship geometry above the bulkhead deck and, as such, it constitutes a major innovation, see Equation (12).

$$Hs_{crit} = \frac{A_{GZ}}{0.5 \cdot GM \cdot Range} \cdot V_R^{\frac{1}{3}} \quad (12)$$

where:

$A_{GZ}$  is the area under the GZ curve (un-truncated).

$GM$  represents the flooded GM.

*Range* represents the range of positive stability.

$V_R$  reflects the residual volume of the watertight envelope (i.e., excluding compartments within the damage extent).

However, severe limitations concerning the choice of parameters, lack of cruise ship data in the formulation, the type of formulation ( $GM$  being a denominator), the interdependence of parameters and lack of demonstrable applicability to grounding damages have limited further application or indeed discussion.

### 3.6. Project eSAFE

eSAFE [30] is the first project where focus on cruise ships has been maintained throughout the research effort. Moreover, this is the first research project in damage stability where all results are based on numerical time-domain simulations for the assessment of the critical

wave height in relation to residual stability parameters. Put differently, numerical simulations were used to generate the requisite statistical information. The simulations have been conducted according to the worst case three-compartment damage lying within 1/3 of the subdivision length about midships and across a range of loading conditions with varying GM values. The dynamic behaviour of each vessel in the damaged condition has been assessed under a range of environmental conditions characterised by varying magnitudes of significant wave height, using a JONSWAP (Joint North Sea Wave Project) spectral shape. For each damage scenario assessed through simulation, the critical significant wave height has been identified, enabling the relationship between the residual stability properties and the critical significant wave height ( $H_{s_{crit}}$ ) to be derived. Based on this information, a new cruise ship-specific formula for predicting the  $H_{s_{crit}}$  has been derived on the basis of GZ properties through regression of the simulation results. Following this, a new s-factor formulation that accounts more accurately for cruise vessels has been proposed using a regression formulation of the significant wave height distribution at the time of accident. The results of two ships of different size indicated that a scaling methodology should also be applied. The most suitable scaling parameter was found to be the “Effective Volume Ratio”; a parameter which accounts for both the scale of the damage and of the vessel. This is an innovation, inspired by project GOALDS. Applying this methodology and populating further the area below 4 metres significant wave height, consistency could be observed.

To ensure that the method is robust and suitable for cruise ships, several additional damages for a whole range of cruise ship size has been analysed. On this basis, the obtained  $H_{s_{crit}}$  formula is provided:

$$H_{s_{crit}} = 7 \cdot \left[ \frac{\min(\lambda \cdot Range, TRange)}{TRange} \cdot \frac{\min(\lambda \cdot GZ_{max}, TGZ_{max})}{TGZ_{max}} \right]^{1.05} \tag{13}$$

where:

$$TGZ_{max} = 0.30 \text{ m.}$$

$$TRange = 30 \text{ degrees.}$$

A formulation for calculating the s-factor was also derived by the regressed CDF (cumulative distribution function) of significant wave heights at the time of collision as follows (in line with HARDER, i.e., up to 4 m):

$$s(H_{s_{crit}}) = 1 - \exp(-1.215 \cdot H_{s_{crit}}) \tag{14}$$

Based on the wave distribution of the global wave statistics, where a 7 m significant wave height represents the 99th percentile, the formula becomes:

$$s(H_{s_{crit}}) = e^{-e^{(1.1717 - 0.9042 \cdot H_{s_{crit}})}} \tag{15}$$

Numerical simulations proved to be consistent with static calculations, in terms of comparing different ships. However, numerical simulation results indicate higher survivability than static calculations, especially in grounding scenarios. In general, it is suggested that the time-domain simulations of flooding within complex geometries require significantly longer simulation runs than the 30 min embedded in SOLAS. Moreover, attempting to capture the complexity of the internal environment in cruise ships, using generalised formulae, has its limitations. It may also be the case that using too many approximations in the attempt to represent reality in the propose generalised formulations of the s-factor and, in all of these, trying to err on the side of safety might lead to conservatism in the results, as shown in Figures 6 and 7.

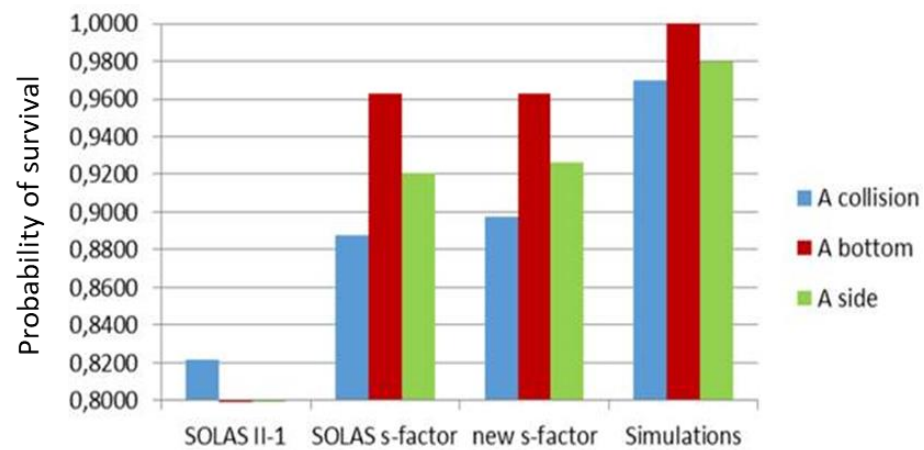


Figure 6. Comparison between static and dynamic assessment—Ship A.

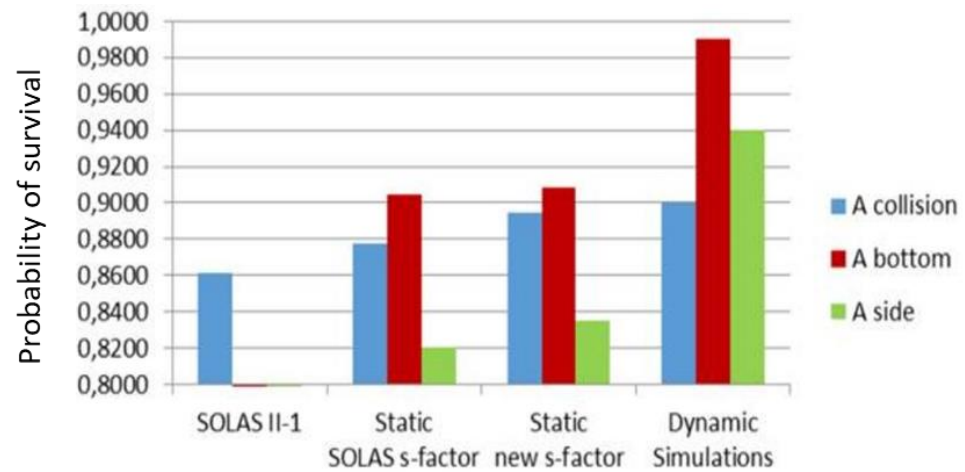


Figure 7. Comparison between static and time-domain simulations results—Ship C.

The main conclusion from the eSAFE project is that the statistical approach does not provide enough granularity to assess the survivability of cruise ships by a statistical approach. This formed the basis and the inspiration for embarking on Project FLARE (flooding accident response) and for exploring in some detail a direct approach for estimating damage survivability of passenger ships, using numerical time-domain simulations.

#### 4. Flooding Risk Quantification

##### 4.1. High-Level Risk Models

This section provides the basis for quantification of the new high-level flooding risk models using the new accident database developed in the EC-funded Project FLARE [31], where the dataset of three hazards, namely collision, side grounding and bottom grounding is utilised. One of the objectives in developing an accident database is to provide input to different nodes/branches in related event trees, which have customarily been used by the maritime industry for flooding risk assessment. Figures 8 and 9 show the different nodes (or high-level event sequences) followed in previous EC-funded projects, specifically GOALDS [12], EMSA III [32] and eSAFE [30]. These models use largely accident statistics and assumptions based on expert judgment to inform/quantify different nodes in the risk models (such as sinking/capsizing and ensuing consequences).

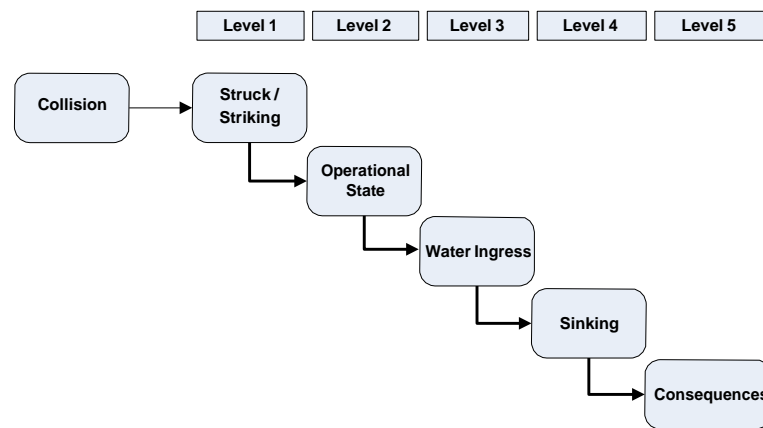


Figure 8. High-level event sequence for collision risk model.

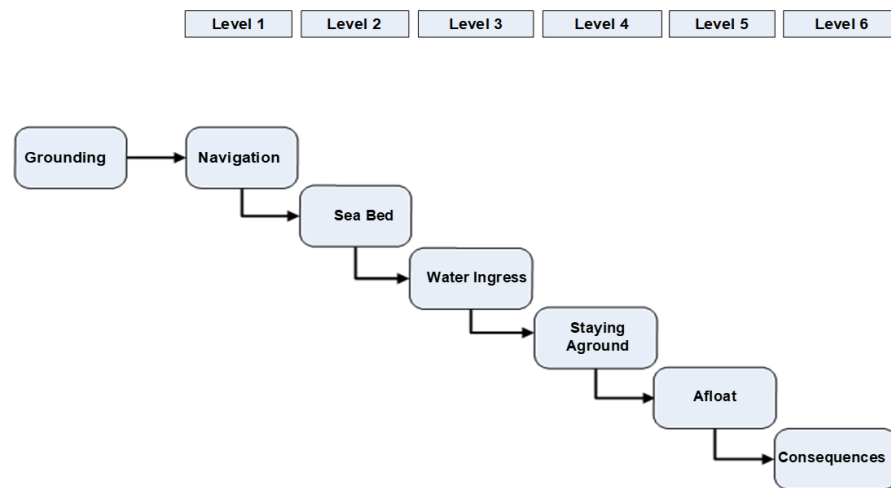


Figure 9. High-level event sequence for grounding risk model.

Finally, Figure 10 shows the high-level structure of an influence model developed in project FLARE [31] to guide the development of pertinent event trees. A noticeable difference is that, unlike previous high level risk models, where the risk model starts with accident type (i.e., collision or grounding), the node ‘operational area’ is now placed before the accident type in the new model. In addition, emphasis is placed on the quantification of different nodes using numerical simulation tools. For instance, for the node probabilities for ‘damage extent’ and their corresponding ‘survival’, the model suggests using the formulation for the “p-factors”, the “s-factors” and the A-Index in SOLAS 2009/2020, the non-zonal approach for collision developed in eSAFE [33,34] and numerical flooding simulations tools for collision and grounding accidents, following suitable verification. For grounding accidents, the probabilities are evaluated based on damage breach probabilistic models and the “non-zonal” approach for the calculation of the corresponding A-Indices [35,36], developed in the framework of EMSA III as well as numerical flooding simulations, the latter again constituting one of the FLARE targets. In addition, the node ‘consequences’ relating to fatalities is evaluated based on the GOALDS/EMSA III assumptions for fast/slow sinking and the corresponding fatality rates based on experiential knowledge. These are substituted in FLARE by using direct risk assessment.

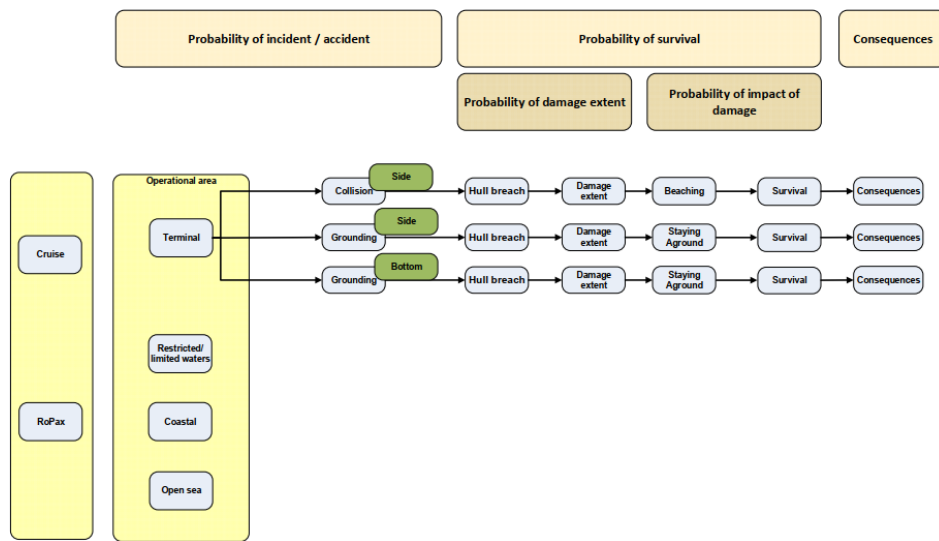


Figure 10. High-level structure of an influence model guiding the development of high level flooding risk models.

Figures 11 and 12 show the different levels or filters used for the collision and grounding high level risk models employed in project FLARE.

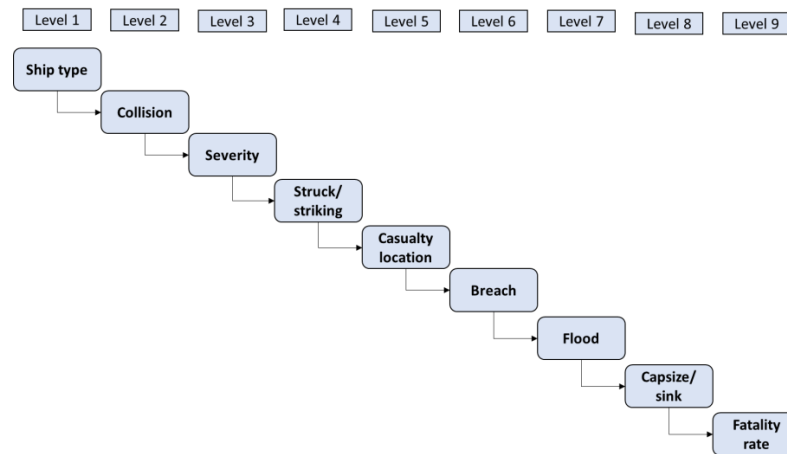


Figure 11. High-level event sequences in the current FLARE collision risk model.

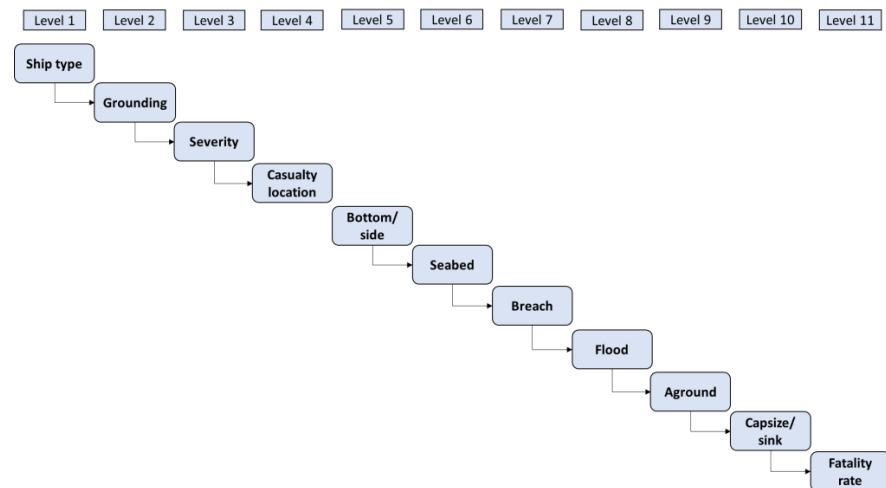


Figure 12. High-level event sequences in the current FLARE grounding risk model.

For collision, nine distinguished levels have been considered, while for grounding 11 levels have been used. The basic structure of the risk model has followed that from GOALDS/EMSA III models, with various updates guided by the new dataset in the FLARE accident database and on direct flooding risk assessment. For instance, ‘damage extent’ and ‘consequences’ in terms of fatalities corresponding to slow and fast sinking is updated with relevant developments in FLARE related to new damage breach distributions and ensuing direct assessments using verified numerical tools. A brief explanation of the different nodes is provided next.

#### 4.1.1. Level 1: Ship Type

The first node in the risk model is assigned to ship type to distinguish the risk model for two types of passenger ships, namely Cruise ship and RoPax. Presently, the category ‘Cruise’ includes Cruise and Pure passenger ships, whereas ‘RoPax’ includes RoRo passenger ships and Rail.

#### 4.1.2. Level 2: Accident Type

In the development of any risk model, in accordance with IMO FSA, the identification of hazards leading to ship flooding is the initial step in the risk model. In this respect, three hazards are considered, namely collision, side grounding and bottom grounding. Side and bottom groundings are considered as a single node (level 5: bottom/side in Figure 12) in the grounding risk model, which again could be further differentiated based on results from pertinent numerical simulations.

#### 4.1.3. Level 3: Severity

For a given hazard and ship type, the severity of the accident is addressed in the form of the node ‘severity’. In general, five potential classes of severity can be identified, as shown in Figure 13. In the risk model, stages 1 and 2 (incident and non-serious) have been grouped into ‘non serious’, and stages 3, 4 and 5 (serious, flood and sink) into ‘serious’ category as only ‘serious’ accidents are considered in project FLARE for risk assessment.

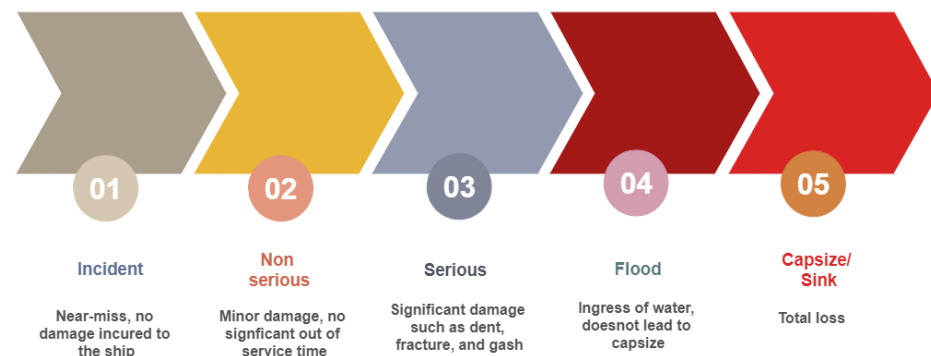


**Figure 13.** Classification of severity of ship flooding accidents.

For the remaining nodes, a similar structure to GOALDS/EMSA III models has been used, as explained next.

#### 4.1.4. Level 4: Struck/Striking Ship (Collision)

Following the GOALDS/EMSA III high level risk model for collision, a struck passenger ship is considered whilst the striking ship is filtered out in serious accidents. Again, further differentiation could be employed, using pertinent numerical tools.

#### 4.1.5. Operational Area (Collision and Grounding)

Following previous high level risk models, ship casualties in three operational areas have been identified for collision and grounding – open sea (at sea), terminal waters (such as port/harbour /dock/etc.) and restricted/limited waters. This follows the same

categorisation used in the data taxonomy in the FLARE accident database. Three nodes are used to differentiate areas of ship operation—terminal, restricted/limited waters and at sea (or open sea) instead of four categories—terminal, restricted/limited waters, coastal waters and at sea (or open sea), as in earlier models, consistent with the taxonomy used in the accident database as there is no sufficient data to feed a higher granularity in the model.

#### 4.1.6. Hull Breach and Water Ingress

These two nodes consider the probability of hull breach and water ingress for collision, side and bottom grounding accidents in three different operational areas.

#### 4.1.7. Capsize/Sink

The probability of capsizing/sinking is determined in previous models based on the value of A-index. In this respect, the same A-index value has been used for ships damaged in different operational areas, and, as such, several critical parameters are not considered. In FLARE, the casualty data are further filtered out, based on a direct method of assessment (survivability index and p-factors, developed in FLARE) for related operational areas and corresponding hull breach.

#### 4.1.8. Fatality Rate

The node ‘consequence’ in the existing models is replaced with ‘fatality rate’ in the current model. For the ship capsizing/sinking, the fatalities and people on board (PoB) are evaluated directly from the accident database to estimate the fatality rate. Therefore, the node ‘fast/slow sinking’ in case of capsizing, used in previous studies, is not considered here. In FLARE, instead of using the same assumed values as in GOALDS/EMSA III models, irrespective of operational area, the quantification of this node will derive from a direct assessment using numerical simulation tools.

At this stage of development, the number of accident cases in each node is estimated to obtain their conditional (dependent) probabilities and the consequence in terms of percentage of fatalities (fatality rate) with respect to the people on board (POB) (where ship capsizing/sinking occurred).

Different nodes in the risk models are quantified using the data from the accident database [37]. In this respect, the following filters are employed to extract the casualty data and fleet at risk:

- Accident period: 1999-01-01 to 2020-10-31 (last 20 years).
- Accident type: Collision and grounding (side and bottom groundings).
- Ship size: gross tonnage (GT)  $\geq$  3500.
- Ship length (overall):  $\geq$  80 m.
- Ship type: Cruise, RoPax, Pure passenger and RoPax (Rail).
- Location: Worldwide.
- Class type: IACS and non-IACS (the latter, for the fleet at risk).

The initial frequencies (probabilities) in the risk models are calculated based on a detailed analysis of fleet at risk data. Accordingly, the IHS Sea-web ‘Ships’ module has been utilised and the same filters, as mentioned earlier, are used to derive fleet data. Figure 14 shows the annual distribution of ship years for different passenger ship types. As mentioned earlier, two ship-type categories have been used—Cruise and RoPax., the former relating to cruise and pure passenger ships and the latter relating to RoPax and RoPax (Rail), with all relevant data merged accordingly. Table 1 provides initial frequencies calculated for collision and grounding events with serious casualties. The data shows that the initial frequency is highest for RoPax ships involved in grounding accidents and lowest for cruise ships involved in collision accidents.

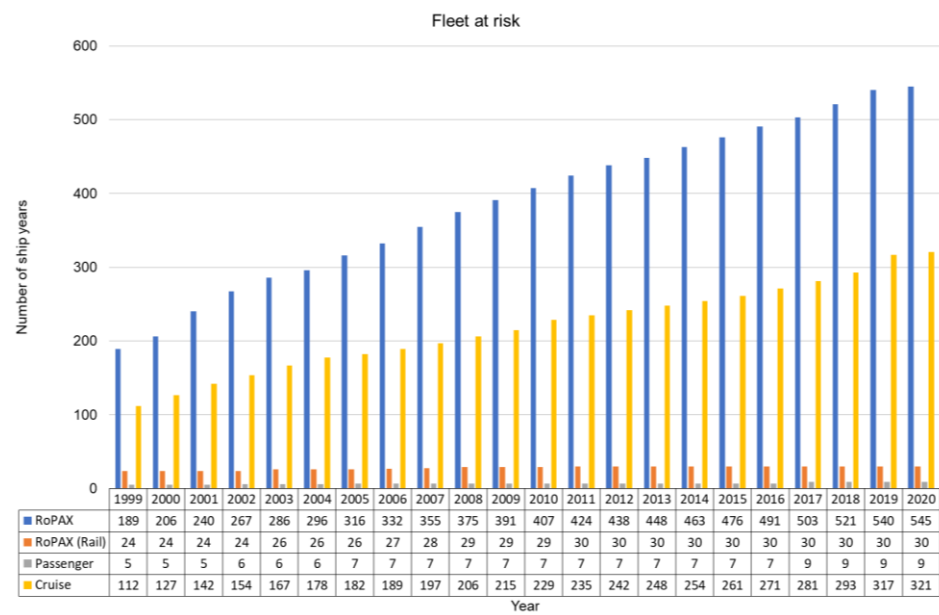


Figure 14. Yearly distribution of the number of fleets registered for different types of passenger ships.

Table 1. Initial accident frequencies of RoPax and cruise ships for different accident types.

Accident Type	No. of Casualties		Fleet at Risk		Initial Frequency		
	RoPax	Cruise	RoPax	Cruise	RoPax	Cruise	Passenger Ships (RoPax and Cruise)
Collision	59	9	9125	4974	$6.47 \times 10^{-3}$	$1.81 \times 10^{-3}$	$8.28 \times 10^{-3}$
Grounding	120	44			$1.32 \times 10^{-2}$	$8.85 \times 10^{-3}$	$2.2 \times 10^{-2}$

Table 2 summarises the total number of accidents for collision, side and bottom grounding scenarios obtained for Cruise and RoPax, separately and collectively. To estimate the effect of combined accident type on ship safety, relative fractions ( $Pr_i$ ) of the accident types are calculated, which may be considered as weighting factors of A-indices following the eSAFE proposal [30], i.e.,:

$$A = Pr_{CL} \cdot A_{CL} + Pr_{GR-S} \cdot A_{GR-S} + Pr_{GR-B} \cdot A_{GR-B} \tag{16}$$

Table 2. Total number of accidents recorded and their respective weighting factors (irrespective of whether there is flooding).

Ship Type	Collision (CL)	Side Grounding (GR-S)	Bottom Grounding (GR-B)	$Pr_{CL}$	$Pr_{GR-S}$	$Pr_{GR-B}$
RoPax	59	50	70	0.330	0.279	0.391
Cruise	9	15	29	0.170	0.283	0.547
Total	68	65	99	0.293	0.280	0.427

Table 3 provides similar results but only for those cases that involve serious flooding.

**Table 3.** Total number of accidents involving flooding and their respective weighting factors.

Ship Type	Collision (CL)	Side Grounding (GR-S)	Bottom Grounding (GR-B)	Pr <sub>CL</sub>	Pr <sub>GR-S</sub>	Pr <sub>GR-B</sub>
RoPax	15	25	21	0.246	0.410	0.344
Cruise	1	12	8	0.048	0.571	0.381
Total	16	37	29	0.208	0.481	0.377

This yields the following expressions for cruise ships and RoPax:

$$A_{Total\_RoPax} = 0.33A_{CL} + 0.28A_{GR-S} + 0.39A_{GR-B} \tag{17}$$

$$A_{Total\_Cruise} = 0.17A_{CL} + 0.28A_{GR-S} + 0.55A_{GR-B} \tag{18}$$

On the basis that flooding is a taxonomizing factor, the respective weighting factors now become:

$$A_{Flood\_RoPax} = 0.25A_{CL} + 0.41A_{GR-S} + 0.34A_{GR-B} \tag{19}$$

$$A_{Flood\_Cruise} = 0.05A_{CL} + 0.57A_{GR-S} + 0.38A_{GR-B} \tag{20}$$

This indicates that flooding incidents due to collision are the minority for both ship types and, for cruise, only a very small contribution (5%), indicating that current SOLAS is misrepresenting the real flooding risk, especially for cruise ships.

The results of the high-level risk models with different nodes and their associated probabilities for collision and grounding events for cruise and RoPax ships, based on the FLARE accident database [37], are described in detail in [38]. Therefore, the risk model is different for Cruise and RoPax ships. Finally, in calculating the accident cases for different nodes, unknown/unspecified information in the dataset was disregarded.

#### 4.2. Risk-Based Safety Metric—SM (eSAFE)

This relates to the safety metric developed in eSAFE, which is updated here based on the new findings as reported in the foregoing. The reference risk models are relevant to both cruise ships and RoPax, the latter based on work conducted in FLARE. On this basis, the potential loss of life (PLL) associated with each type of accident can be determined as follows:

$$\begin{aligned} PLL_{CL} &= POB \cdot c_{CL} \cdot (1 - A_{CL}) \\ PLL_{GR-B} &= POB \cdot c_{GR-B} \cdot (1 - A_{GR-B}) \\ PLL_{GR-S} &= POB \cdot c_{GR-S} \cdot (1 - A_{GR-S}) \end{aligned} \tag{21}$$

where, *POB* is the number of persons on board (crew and passengers, considering assumptions with respect to occupancy). The coefficients *c<sub>CL</sub>*, *c<sub>GR-B</sub>* and *c<sub>GR-S</sub>* can be directly calculated from Equations (25) and (26). The total PLL (*PLL<sub>TOT</sub>*) can be obtained by summing up the risk contributions from the three types of accidents, i.e.:

$$\begin{aligned} PLL_{TOT} &= PLL_{CL} + PLL_{GR-B} + PLL_{GR-S} \\ &= POB \cdot [c_{CL} \cdot (1 - A_{CL}) + c_{GR-B} \cdot (1 - A_{GR-B}) + c_{GR-S} \cdot (1 - A_{GR-S})] \end{aligned} \tag{22}$$

*PLL<sub>TOT</sub>* represents the risk associated with a vessel with given *POB* and attained indices *A<sub>CL</sub>*, *A<sub>GR-B</sub>* and *A<sub>GR-S</sub>*, as measured based on the assumed reference risk models Equations (19) and (20) for cruise ships and RoPax, respectively. The total societal risk

$PLL_{TOT}$  can be reformulated, leading to what is denoted as  $SM$ , which combines the impact from all three types of accidents, as follows:

$$\begin{cases} SM = k_{CL} \cdot A_{CL} + k_{GR-B} \cdot A_{GR-B} + k_{GR-S} \cdot A_{GR-S} \\ PLL_{TOT} = POB \cdot c_T \cdot (1 - SM) \\ \text{where} \\ c_T = c_{CL} + c_{GR-B} + c_{GR-S} \\ k_{CL} = \frac{c_{CL}}{c_T} ; k_{GR-B} = \frac{c_{GR-B}}{c_T} ; k_{GR-S} = \frac{c_{GR-S}}{c_T} \end{cases} \quad (23)$$

It also follows that contributions to  $PLL_{TOT}$  from different types of accidents (collision, bottom and side grounding) can be expressed as follows:

$$\begin{cases} PLL_{TOT} = PLL_{CL} + PLL_{GR-B} + PLL_{GR-S} \\ \text{where} \\ PLL_{CL} = POB \cdot c_T \cdot k_{CL} \cdot (1 - A_{CL}) \\ PLL_{GR-B} = POB \cdot c_T \cdot k_{GR-B} \cdot (1 - A_{GR-B}) \\ PLL_{GR-S} = POB \cdot c_T \cdot k_{GR-S} \cdot (1 - A_{GR-S}) \end{cases} \quad (24)$$

The main characteristic of this procedure is that the resulting weighting factors  $k_{CL}$ ,  $k_{GR-B}$  and  $k_{GR-S}$  for the three attained indices in the safety metric  $SM$ , are considering the relative contribution to risk stemming from different types of accidents with reference to cruise ships and RoPax. In this way, types of accident providing a large contribution to risk also provide a corresponding greater contribution in the combined safety metric  $SM$ . Numerical values of the coefficients are summarised in Table 4, from which:

$$SM_{Cruise\_ships} = 0.05A_{CL} + 0.38A_{GR-B} + 0.57A_{GR-S} \quad (25)$$

$$SM_{RoPax\_ships} = 0.25A_{CL} + 0.34A_{GR-B} + 0.41A_{GR-S} \quad (26)$$

**Table 4.** Risk-based safety metric  $SM$  for cruise ships and RoPax, based on FLARE risk models.

	$k_{CL}$ (-)	$k_{GR-B}$ (-)	$k_{GR-S}$ (-)	$c_T$ (1/Ship-Year)
Cruise	0.05	0.38	0.57	$1.07 \times 10^{-2}$
RoPax	0.25	0.34	0.41	$1.96 \times 10^{-2}$

$$\begin{cases} SM = k_{CL} \cdot A_{CL} + k_{GR-B} \cdot A_{GR-B} + k_{GR-S} \cdot A_{GR-S} \\ PLL_{TOT} = POB \cdot c_T \cdot (1 - SM) = PLL_{CL} + PLL_{GR-B} + PLL_{GR-S} \\ PLL_{CL} = POB \cdot c_T \cdot k_{CL} \cdot (1 - A_{CL}) \\ PLL_{GR-B} = POB \cdot c_T \cdot k_{GR-B} \cdot (1 - A_{GR-B}) \\ PLL_{GR-S} = POB \cdot c_T \cdot k_{GR-S} \cdot (1 - A_{GR-S}) \end{cases}$$

This concept, which has been summarised for the case of global indices, can be similarly applied to obtain safety metrics  $SM$  for each calculation draught by using corresponding partial A-indices.

### 5. Concluding Remarks

Despite a late start and slow early development in the subject of probabilistic damage stability and flooding risk assessment, the past three decades have seen remarkable progress in the evolutionary development of these subjects. Contributing factors towards the slow early pace and the latter step changes include the following:

- Lack in contemporary knowledge, methods and tools for a direct assessment of damage stability and ensuing risk on a ship- and accident-specific basis.

- The need to ensure inbuilt resilience in ship design to limit catastrophic consequences fuelled an approach based on accidents statistics with damage limitation in mind.
- The need to rationalise such an approach for application to all ship types and with focus only on new buildings, made such an approach progressively less relevant and, ultimately, too abstract. This, in turn, necessitated ship-specific developments and, ultimately a better understanding of the limitations, fuelling focus on direct assessment methods with tangible benefits, yet to be fully realised.
- Generally speaking, there is a consistent methodology underlying such development over the past half a century.
- The focus is now clear and the effort more targeted rendering the subject sound from a research perspective whilst providing a platform for exciting new ship designs and safer operation.

**Author Contributions:** Conceptualization, D.V. and M.P.M.-A.; methodology, D.V. and M.P.M.-A.; formal analysis, D.V. and M.P.M.-A.; investigation, D.V. and M.P.M.-A.; data curation, D.V. and M.P.M.-A.; writing—original draft preparation, D.V. and M.P.M.-A.; writing—review and editing, D.V. and M.P.M.-A.; supervision, D.V. All authors have read and agreed to the published version of the manuscript.

**Funding:** This research received funding from European Union project FLARE (Flooding Accident Response) project, grant number 814753, under H2020 program.

**Institutional Review Board Statement:** Not applicable.

**Informed Consent Statement:** Not applicable.

**Acknowledgments:** The authors should like to acknowledge all our researcher friends and industry colleagues who contributed to the sustained evolution of the damage stability subject.

**Conflicts of Interest:** The authors declare no conflict of interest. The views presented in the paper are those of the authors alone.

## References

1. Vassalos, D.; Guarin, L. Designing for damage stability and survivability—Contemporary developments and implementation. *Ship Sci. Technol.* **2009**, *1*, 59–71.
2. IMO. *SOLAS-International Convention for the Safety of Life at Sea*; IMO: London, UK, 2009.
3. Wendel, K. Die Wahrscheinlichkeit des Uberstehens von Verletzungen. *Schiffstechnik* **1960**, *7*, 47–61.
4. Wendel, K. Subdivision of ships. In Proceedings of the 1968 Diamond Jubilee International Meeting—75th Anniversary; Paper No. 12. SNAME: New York, NY, USA, 1968; p. 27.
5. Zhang, M.; Conti, F.; Vassalos, D.; Kujala, P.; Lindroth, D.; Hirdaris, S. Direct assessment of ship collision damage and flooding risk. *Ocean Eng.* **2020**, accepted.
6. Vassalos, D.; Paterson, D. Towards unsinkable ships. *Ocean Eng.* **2021**, *232*, 109096. [[CrossRef](#)]
7. Vassalos, D.; Jasionowski, A.; Dodworth, K.; Allan, T.; Matthewson, B. *Time-based Survival Criteria for Ro-Ro Vessels*; RINA Spring Meetings: London, UK, 1998.
8. Vassalos, D.; Turan, O.; Pawlowski, M. Dynamic stability assessment of damaged ships and proposal of rational survival criteria. *J. Mar. Technol.* **1997**, *34*, 241–269.
9. Tsakalakis, N.; Cichowicz, J.; Vassalos, D. The concept of the capsizing band revisited. In Proceedings of the 11th International Ship Stability Workshop, Wageningen, The Netherlands, 21–23 June 2010.
10. Jasionowski, A. *Study of the Specific Damage Stability Parameters of Ro-Ro Passenger Vessels According to SOLAS 2009 Including Water on Deck Calculation*; European Maritime Safety Agency: Lisbon, Portugal, 2009.
11. Jasionowski, A. *Study of the Specific Damage Stability Parameters of Ro-Ro Passenger Vessels According to SOLAS 2009 Including Water on Deck Calculation. 2nd EMSA Study on Damage Stability of RoPax Vessels, Project No EMSA/OP/08/2009*; Ship Stability Research Centre, University of Strathclyde: Strathclyde, UK, 2009.
12. GOALDS. Goal-Based Damage Stability. In *Project funded by the European 13th Commission, FP7- DG Research, Grant Agreement 233876*; IMO Publishing: London, UK, 2009–2012.
13. HARDER. *Harmonisation of Rules and Design Rationale*; EC Contact No. GDRB-CT-1998-00028, Final Technical Report; IMO Publishing: London, UK, 1999–2003.
14. Cichowicz, J.; Tsakalakis, N.; Vassalos, D.; Jasionowski, A. Damage survivability of passenger ships—Re-engineering the safety factor. *Safety* **2016**, *2*, 4. [[CrossRef](#)]

15. IMCO. *Resolution A.265 VIII, Regulations on Subdivision and Stability of Passenger Ships as Equivalent to Part B of Chapter II of the International Convention for the Safety of Life at Sea, 1960*; IMCO: London, UK, Adopted November 1973.
16. Bird, H.; Browne, R. *Damage Stability Model Experiments*; 0035-8967; RINA: Genoa, Italy, 1973; Volume 116, pp. 69–91.
17. Middleton, E.; Numata, E. *Tests of a Damaged Stability Model in Waves*; SNAME Transactions: Washington, DC, USA, 1970.
18. Vassalos, D.; Papanikolaou, A. Stockholm Agreement—Past, Present and Future (Part 2). *Mar. Technol.* **2002**, *39*, 137–158,199–210.
19. Vassalos, D.; Pawlowski, M.; Turan, O. Criteria for survival in damaged condition. In *Ship Hydromechanics and Structures*; Delft Technical University: Wageningen, The Netherlands, 1995.
20. Tagg, R.; Tuzcu, C. A Performance-based Assessment of the Survival of Damaged Ships—Final Outcome of the EU Research Project HARDER. In Proceedings of the 6th International Ship Stability Workshop (ISSW), New York, NY, USA, 13–16 October 2002.
21. IMO. *Resolution 14 Agreement Concerning Specific Stability Requirements for Ro-Ro Passenger Ships Undertaking Regular Scheduled International Voyages Between or To or From Designated Ports in North West Europe and the Baltic Sea*; IMO: London, UK, 1996.
22. Tuzcu, C. Development of factors: The damage survival probability. In Proceedings of the 8th International Conference on the Stability of Ships and Ocean Vehicles (STAB2003), Madrid, Spain, 15–19 September 2003.
23. Jasionowski, A. *Survival Criteria for Large Passenger Ships*; SAFENVSHIP Project, Final Report; Safety at Sea Ltd.: Glasgow, UK, 2005.
24. Vassalos, D.; York, A.; Jasionowski, A.; Kanerva, M.; Scott, A. Design implications of the new harmonised probabilistic damage stability regulations. *Int. Shipbuild. Prog.* **2007**, 339–361.
25. Vassalos, D.; Jasionowski, A. SOLAS 2009—Raising the Alarm. In *Contemporary Ideas on Ship Stability and Capsizing in Waves*; Neves, M., Ed.; Springer: Berlin/Heidelberg, Germany, 2011.
26. Spanos, D.; Papanikolaou, A. Considerations on the survivability assessment of damaged ships. In Proceedings of the 12th International Ship Stability Workshop (ISSW2011), Washington, DC, USA, 12–15 June 2011.
27. Pawlowski, M. Developing the s-factor. In Proceedings of the 10th International Conference on Stability of Ships and Ocean Vehicles (STAB2009), St. Petersburg, Russia, 22–26 June 2009.
28. Heimvik, N. *Wave Height Distribution According to Damage Statistics*; HARDER (Harmonisation of Rules and Design Rationale) project No: GRD1-1999-10721, Report No: 3-33-W-2001-01-0; DNV: Hovik, Norway, 2001.
29. Tagg, R. Comparison of survivability between SOLAS 90/95 and SOLAS 2009 ships—A retrospective view of 10 years on from project HARDER. In Proceedings of the 14th International Ship Stability Workshop (ISSW2014), Kuala Lumpur, Malaysia, 29 September–1 October 2014.
30. Luhmann, H.; Bulian, G.; Vassalos, D.; Olufsen, O.; Seglem, I.; Pottgen, J. eSAFE-D4.3.2—Executive Summary, Joint Industry Project eSAFE-Enhanced Stability After a Flooding Event—A Joint Industry Project on Damage Stability for Cruise Ships. Cruise Ship Safety Forum (CSSF), 2018. Available online: <https://cssf.cruising.org/references?rq=esafe> (accessed on 20 May 2021).
31. FLARE. EU H2020—MG2.2 Flooding Accident Response. 2019–2022. Available online: <https://flare-project.eu/> (accessed on 14 June 2021).
32. European Maritime Safety Agency. *EMSA III/OP/10/2013: Risk Level and Acceptance Criteria for Passenger Ships*; DNV GL: Hovik, Norway, 2014.
33. Bulian, G.; Cardinale, M.; Francescutto, A.; Zaraphonitis, G. Complementing SOLAS damage ship stability framework with a probabilistic description for the extent of collision damage below the waterline. *Ocean Eng.* **2019**, *186*, 106073. [[CrossRef](#)]
34. Bulian, G.; Cardinale, M.; Dafermos, G.; Eliopoulou, E.; Francescutto, A.; Hamann, R.; Lindroth, D.; Luhmann, H.; Ruponen, P.; Zaraphonitis, G. Considering collision, bottom grounding and side grounding/contact in a common non-zonal framework. In Proceedings of the 17th International Ship Stability Workshop (ISSW 2019), Helsinki, Finland, 10–12 June 2019.
35. Bulian, G.; Lindroth, D.; Ruponen, P.; Zaraphonitis, G. Probabilistic assessment of damaged ship survivability in case of grounding: Development and testing of a direct non-zonal approach. *Ocean Eng.* **2016**, *120*, 331–338. [[CrossRef](#)]
36. Bulian, G.; Cardinale, M.; Dafermos, G.; Lindroth, D.; Ruponen, P.; Zaraphonitis, G. Probabilistic assessment of damaged survivability of passenger ships in case of grounding or contact. *Ocean Eng.* **2020**, *218*, 107396. [[CrossRef](#)]
37. Mujeeb-Ahmed, M.P.; Vassalos, D.; Boulougouris, E. Development of collision and grounding accident database for large passenger ships. In Proceedings of the First International Conference on the Stability and Safety of Ships and Ocean Vehicles (STAB&S 2021), Glasgow, UK, 7–11 June 2021.
38. Mujeeb-Ahmed, M.P.; Vassalos, D.; Boulougouris, E. Probabilistic damage distribution and risk modelling of collision and grounding accidents for large passenger ships. In Proceedings of the First International Conference on the Stability and Safety of Ships and Ocean Vehicles (STAB&S 2021), Glasgow, UK, 7–11 June 2021.